



A comparison of gravitational effects between a spherical zonal band and a spherical shell discretized using tesseroids

Xiao-Le Deng¹

¹ Department of Earth and Space Sciences, Southern University of Science and Technology, Shenzhen, 518055, China
(xldeng@whu.edu.cn)



Content



1. Introduction
2. Theory
3. Numerical experiments
4. Conclusion
5. Outlook

1. Introduction

Gravitational effects (e.g. gravitational potential (GP), gravity vector (GV), gravity gradient tensor (GGT), and gravitational or gravity curvatures (GC))

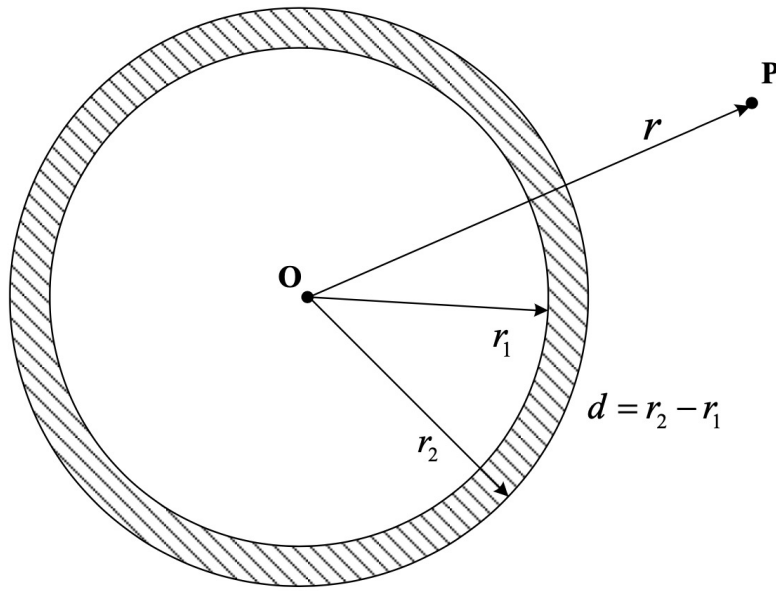


Fig. 1 Spherical shell

Revised from Deng and Shen (2018)

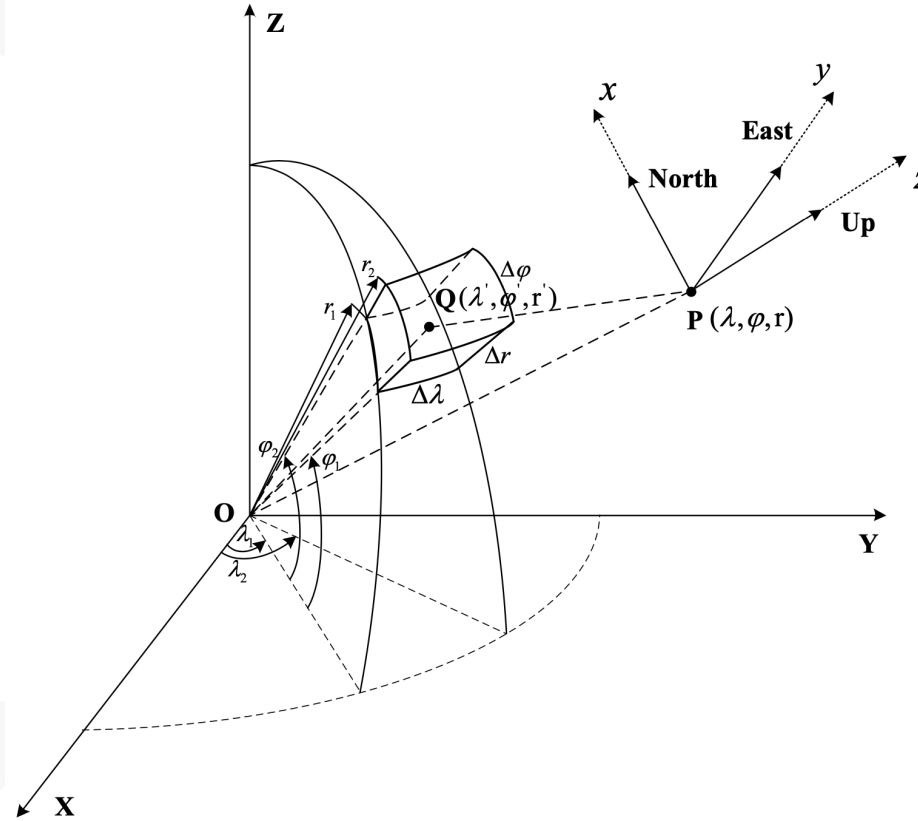


Fig. 2 Tesseroid

Revised from Deng and Shen (2009)

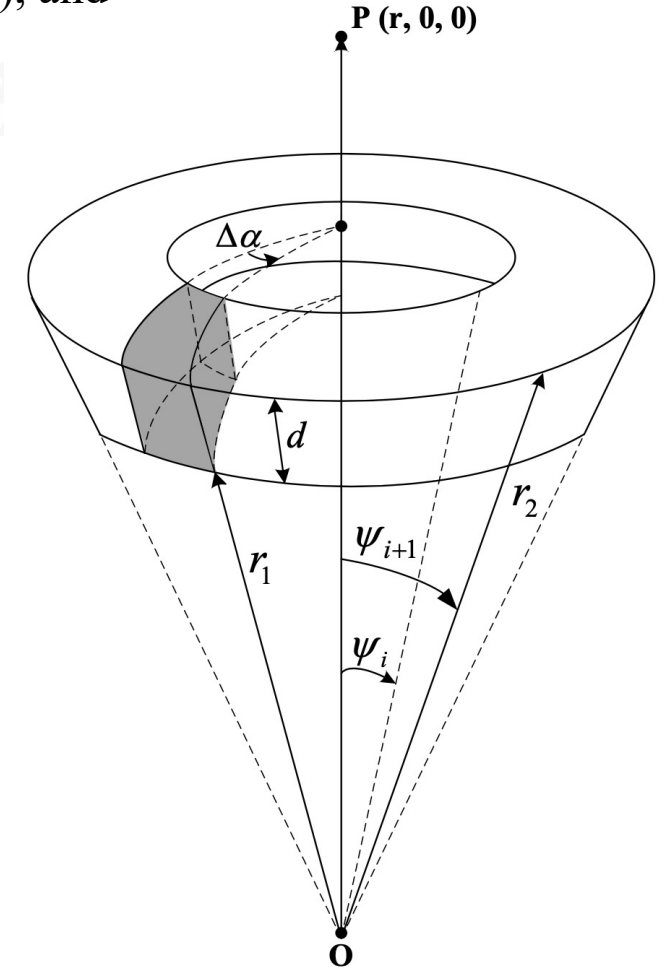
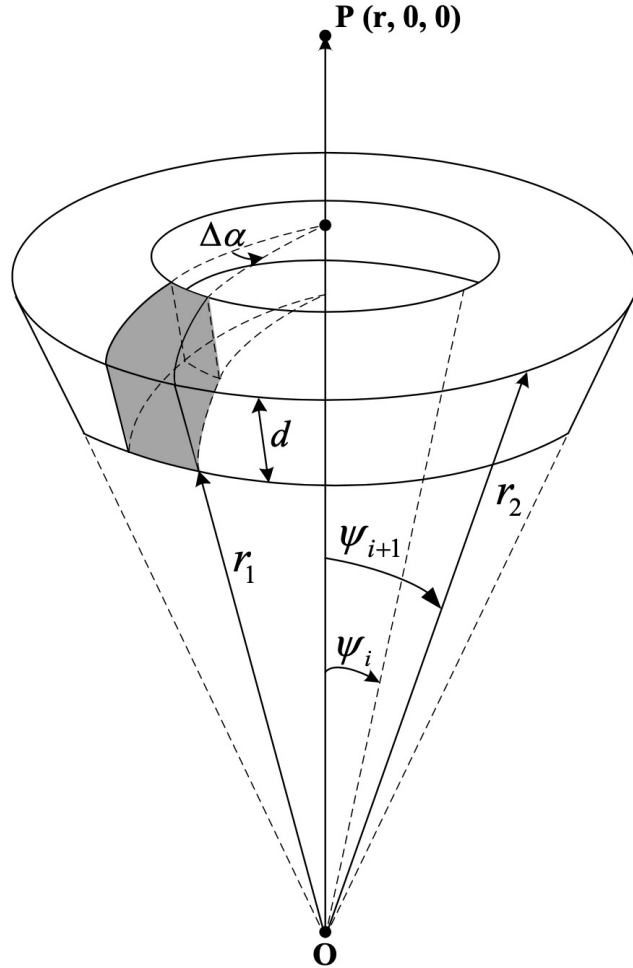


Fig. 3 Spherical zonal band

Revised from Heck and Seitz (2007)

2. Theory: gravitational effects of a spherical cap



The formula of the Gravitational Potential (GP) of a spherical cap is presented as (Papp and Wang 1996; Heck and Seitz 2007):

$$V(r; r_1, r_2, \psi_c) = 2\pi G\rho \left[\frac{1}{3r} \ell_c'^3 + \frac{1}{2} \ell_c' \cos \psi_c (r' - r \cos \psi_c) + \frac{1}{2} r^2 \cos \psi_c \sin^2 \psi_c \ln(\ell_c' + r' - r \cos \psi_c) \right] \Big|_{r'=r_1}^{r'=r_2} \quad (1)$$

$$+ 2\pi G\rho \left(+ \frac{1}{3r} r'^3 - \frac{1}{2} r'^2 \right) \Big|_{r'=r_1}^{r'=r_2} \begin{cases} +1 & r \geq r_2 \\ -1 & r \leq r_1 \end{cases}$$

$$\ell_c' = \sqrt{r^2 + r'^2 - 2rr' \cos \psi_c} \quad (2)$$

Fig. 3 Spherical zonal band

Revised from Heck and Seitz (2007)

2. Theory



Gravity Vector (GV: V_x , V_y , V_z) and
Gravity Gradient Tensor
(GGT: V_{xx} , V_{xy} , V_{xz} , V_{yy} , V_{yz} , V_{zz})
of a spherical cap

$$V_x(r; r_1, r_2, \psi_c) = V_y(r; r_1, r_2, \psi_c) = 0 \quad (3)$$

$$\begin{aligned} V_z(r; r_1, r_2, \psi_c) &= \frac{\partial V(r; r_1, r_2, \psi_c)}{\partial r} \\ &= 2\pi G\rho \left\{ \frac{1}{6r^2} \left[\ell'_c(r^2 - 3r^2 \cos 2\psi_c - 2r'^2) \right. \right. \end{aligned} \quad (4)$$

v.s. Eq. (54) of Heck and Seitz (2007)

$$\left. + r \cos \psi_c \left[3r^2 \sin^2 \psi_c [2 \ln(\ell'_c + r' - r \cos \psi_c) + 1] - 2\ell'_c r' \right] \right\} \Big|_{r'=r_1}^{r'=r_2} + 2\pi G\rho \left(-\frac{r'^3}{3r^2} \right) \Big|_{r'=r_1}^{r'=r_2} \begin{cases} +1 & r \geq r_2 \\ -1 & r \leq r_1 \end{cases}$$

$$V_{xy}(r; r_1, r_2, \psi_c) = V_{xz}(r; r_1, r_2, \psi_c) = V_{yz}(r; r_1, r_2, \psi_c) = 0 \quad (5)$$

$$\begin{aligned} V_{zz}(r; r_1, r_2, \psi_c) &= \frac{\partial V^2(r; r_1, r_2, \psi_c)}{\partial r^2} = \frac{\partial V_z(r; r_1, r_2, \psi_c)}{\partial r} \\ &= 2\pi G\rho \left\{ \frac{1}{6r^3 \ell'_c} \left[r^4 + 2r^2 r'^2 + 4r'^4 - 2r^2 r'^2 \cos^2 \psi_c \right. \right. \\ &\quad - 3r^4 \cos 2\psi_c - r \cos \psi_c \left[r^2 r' + 4r'^3 - 3r^2 r' \cos 2\psi_c \right. \\ &\quad \left. \left. - 3r^2 \sin^2 \psi_c [2\ell'_c \ln(\ell'_c + r' - r \cos \psi_c) + 3\ell'_c - 2r'] \right] \right] \right\} \Big|_{r'=r_1}^{r'=r_2} \\ &\quad + 2\pi G\rho \left(\frac{2r'^3}{3r^3} \right) \Big|_{r'=r_1}^{r'=r_2} \begin{cases} +1 & r > r_2 \\ -1 & r < r_1 \end{cases} \end{aligned}$$

(6)
v.s. Eq. (19) of Lin et al. (2020)

$$V_{xx}(r; r_1, r_2, \psi_c) = V_{yy}(r; r_1, r_2, \psi_c) = -\frac{1}{2} V_{zz}(r; r_1, r_2, \psi_c) \quad (7)$$



2. Theory

$$\begin{aligned} V_{xxx}(r; r_1, r_2, \psi_c) &= V_{xxy}(r; r_1, r_2, \psi_c) = V_{xyz}(r; r_1, r_2, \psi_c) \\ &= V_{yyx}(r; r_1, r_2, \psi_c) = V_{yyy}(r; r_1, r_2, \psi_c) = V_{zzx}(r; r_1, r_2, \psi_c) \\ &= V_{zzy}(r; r_1, r_2, \psi_c) = 0 \end{aligned} \quad (8)$$

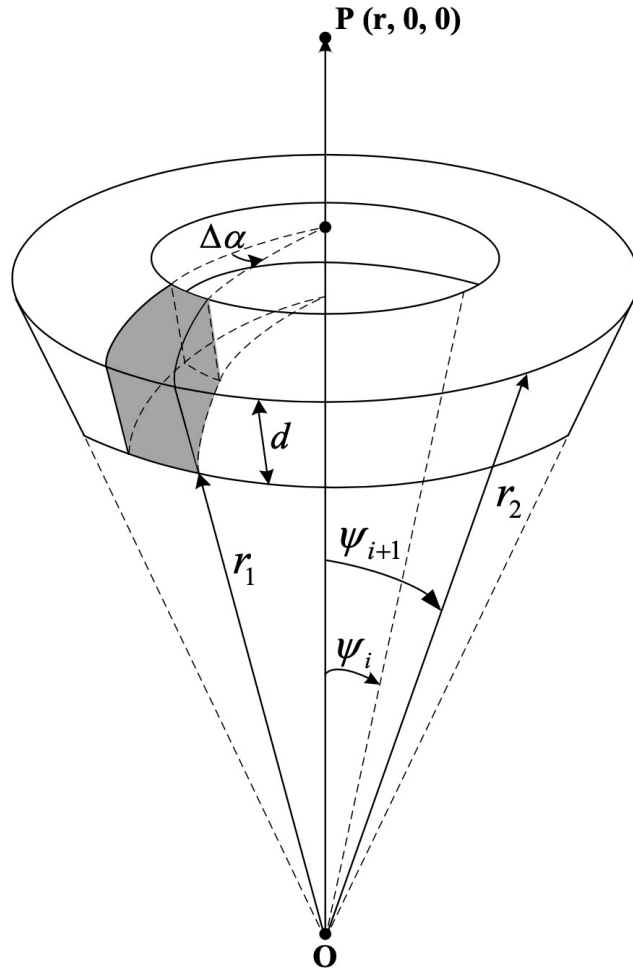
$$\begin{aligned} V_{zzz}(r; r_1, r_2, \psi_c) &= \frac{\partial V^3(r; r_1, r_2, \psi_c)}{\partial r^3} = \frac{\partial V_{zz}(r; r_1, r_2, \psi_c)}{\partial r} \\ &= 2\pi G\rho \left\{ -\frac{1}{8r^4 \ell_c'^3 (\ell_c' + r' - r \cos \psi_c)} \left[4r'(r^6 + 3r^4 r'^2 \right. \right. \\ &\quad + 15r^2 r'^4 + 4r'^6) + \ell_c' (r^6 + 3r^4 r'^2 + 36r^2 r'^4 + 16r'^6) \\ &\quad - 2r \cos \psi_c [2r^4 r' (\ell_c' + 2r') + 3r^2 r'^3 (3\ell_c' + 10r') \\ &\quad + 8r'^5 (3\ell_c' + 4r') + r^6] + r^2 [4r'^3 \cos 2\psi_c (3r' \ell_c' + 9r'^2 + 2r^2) \\ &\quad + r \cos 3\psi_c (3r^2 r' \ell_c' + 6r^2 r'^2 + 2r'^3 \ell_c' - 4r'^4 + 2r^4) \\ &\quad - r^2 \cos 4\psi_c (r^2 \ell_c' + 3r'^2 \ell_c' + 4r^2 r' + 4r'^3) \\ &\quad \left. \left. + r^3 r' \cos 5\psi_c (\ell_c' + 2r') \right] \right\} \Big|_{r'=r_1}^{r'=r_2} \\ &\quad + 2\pi G\rho \left(-\frac{2r'^3}{r^4} \right) \Big|_{r'=r_1}^{r'=r_2} \begin{cases} +1 & r > r_2 \\ -1 & r < r_1 \end{cases} \end{aligned} \quad (9)$$

$$V_{xxz}(r; r_1, r_2, \psi_c) = V_{yyz}(r; r_1, r_2, \psi_c) = -\frac{1}{2} V_{zzz}(r; r_1, r_2, \psi_c) \quad (10)$$

Gravitational Curvatures
(GC: V_{xxx} , V_{xxy} , V_{xxz} , V_{xyz} ,
 V_{yyx} , V_{yyy} , V_{yyz} ,
 V_{zzx} , V_{zzy} , V_{zzz})
of a spherical cap



2. Theory: gravitational effects of a spherical zonal band



$$F(r; r_1, r_2, \psi_i, \psi_{i+1}) = F(r; r_1, r_2, \psi_{i+1}) - F(r; r_1, r_2, \psi_i) \quad (11)$$

$$\begin{aligned} V_{xx}(r; r_1, r_2, \psi_i, \psi_{i+1}) &= V_{yy}(r; r_1, r_2, \psi_i, \psi_{i+1}) \\ &= -\frac{1}{2} \left[V_{zz}(r; r_1, r_2, \psi_{i+1}) - V_{zz}(r; r_1, r_2, \psi_i) \right] \end{aligned} \quad (12)$$

$$\begin{aligned} V_{xxz}(r; r_1, r_2, \psi_i, \psi_{i+1}) &= V_{yyz}(r; r_1, r_2, \psi_i, \psi_{i+1}) \\ &= -\frac{1}{2} \left[V_{zzz}(r; r_1, r_2, \psi_{i+1}) - V_{zzz}(r; r_1, r_2, \psi_i) \right] \end{aligned} \quad (13)$$

Fig. 3 Spherical zonal band

Revised from Heck and Seitz (2007)

3. Numerical experiments

- The relative errors using **tesseroids** to discrete the whole **spherical zonal band** and **spherical shell** are performed by 3D Gauss-Legendre quadrature method (Wild-Pfeiffer 2008; Lin et al. 2020):

$$\delta F = \text{Log}_{10} \left(\left| \frac{\sum F^{\text{tess}}}{F^{\text{ref}}} - 1 \right| \right) \quad (14)$$

Table 1 Numerical values in the experiments

Parameter	Notation	Magnitude	Unit
Newtonian gravitational constant	G	6.673×10^{-11}	$\text{m}^3 \text{kg}^{-1} \text{s}^{-2}$
Up geocentric distance of the spherical cap	r_2	6,378,137	m
Down geocentric distance of the spherical cap	r_1	6,377,137	m
Thickness of the spherical cap	$d = r_2 - r_1$	1,000	m
Height above the surface of the spherical cap	h	260,000	m
Geocentric distance of the computation point P	$r = r_2 + h$	6,638,137	m
Density of the spherical cap	ρ	2,670	kg m^{-3}

- Comparison of computation time between a spherical zonal band and spherical shell discretized using tesserooids in double and quadruple precision with different grid sizes

Table 2 Numerical results of computation time

Grid size	N_band	N_shell	Ratio	GP_d	GV_d	GGT_d	GC_d	All_d	GP_q	GV_q	GGT_q	GC_q	All_q
20° × 20°	18	162	9	6.3	7.5	5.7	5.9	6.3	8.7	8.7	8.8	8.8	8.8
15° × 15°	24	288	12	7.2	9.4	8.3	8.5	8.4	11.7	11.7	11.7	11.7	11.7
10° × 10°	36	648	18	15.9	13.8	13.7	13.8	14.3	17.4	17.9	17.7	17.8	17.7
5° × 5°	72	2,592	36	31.3	33.5	31.7	31.3	31.9	35.7	35.7	35.6	35.5	35.6
3° × 3°	120	7,200	60	53.4	55.3	56.2	55.5	55.1	60.3	59.7	59.2	59.6	59.7
2° × 2°	180	16,200	90	85.7	86.0	83.0	84.6	84.8	89.7	88.7	91.3	89.4	89.8
1° × 1°	360	64,800	180	173.5	174.9	173.9	173.5	174.0	178.7	179.5	179.5	180.1	179.4
30' × 30'	720	259,200	360	333.5	347.8	352.4	354.9	347.2	359.8	360.4	361.5	362.7	361.1
15' × 15'	1,440	1,036,800	720	730.3	719.2	707.0	709.0	716.4	716.4	721.5	725.3	724.9	722.0
10' × 10'	2,160	2,332,800	1,080	1,084.3	1,094.4	1,079.0	1,087.2	1,086.2	1,069.9	1,082.5	1,092.0	1,090.1	1,083.6
5' × 5'	4,320	9,331,200	2,160	2,149.9	2,165.3	2,177.0	2,168.9	2,165.3	2,143.0	2,133.9	2,156.2	2,178.0	2,152.8
3' × 3'	7,200	25,920,000	3,600	3,571.1	3,690.6	3,653.0	3,642.0	3,639.4	3,597.9	3,609.2	3,619.9	3,647.9	3,618.7
2' × 2'	10,800	58,320,000	5,400	5,421.8	5,487.6	5,447.4	5,439.2	5,449.0	5,338.4	5,360.5	5,448.0	5,416.2	5,390.8

$$n^\circ \times n^\circ \quad 180/n$$

- The computation time of a spherical zonal band discretized using tesserooids is about **180/n** times less than that of a spherical shell discretized using tesserooids for gravitational effects (i.e., GP, GV, GGT, and GC) with different grid sizes in double and quadruple precision.

➤ Comparison of computation errors between the tessieroids discretizing a **spherical zonal band** and the tessieroids discretizing a **spherical shell**

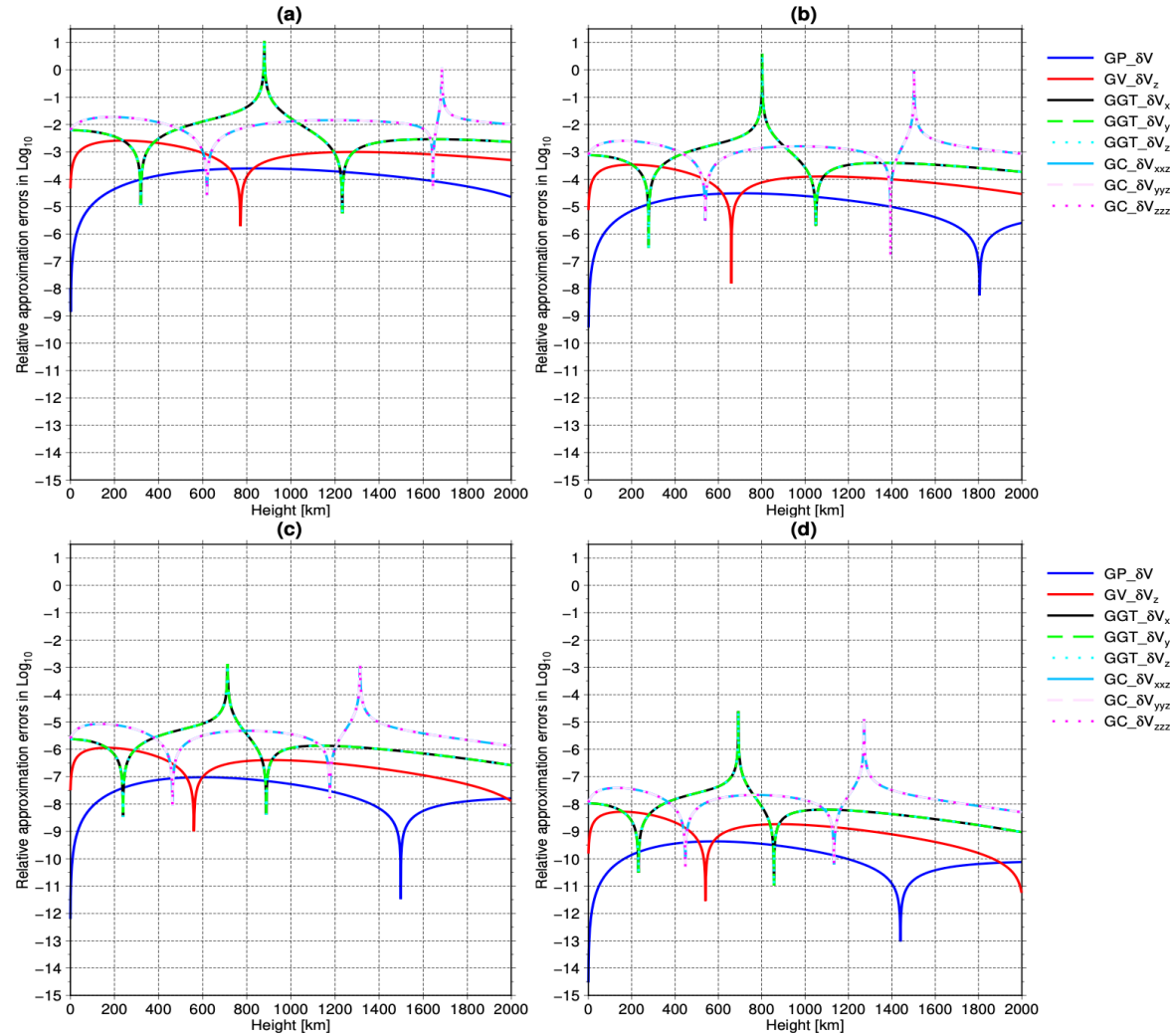


Fig. 4 Relative approximation errors in Log10 scale of nonzero gravitational effects of a **spherical zonal band** discretized using tessieroids with the influence of the computation point's height by a grid size of (a) 10d x 10d, (b) 5d x 5d, (c) 1d x 1d, and (d) 15'x15' in quadruple precision.

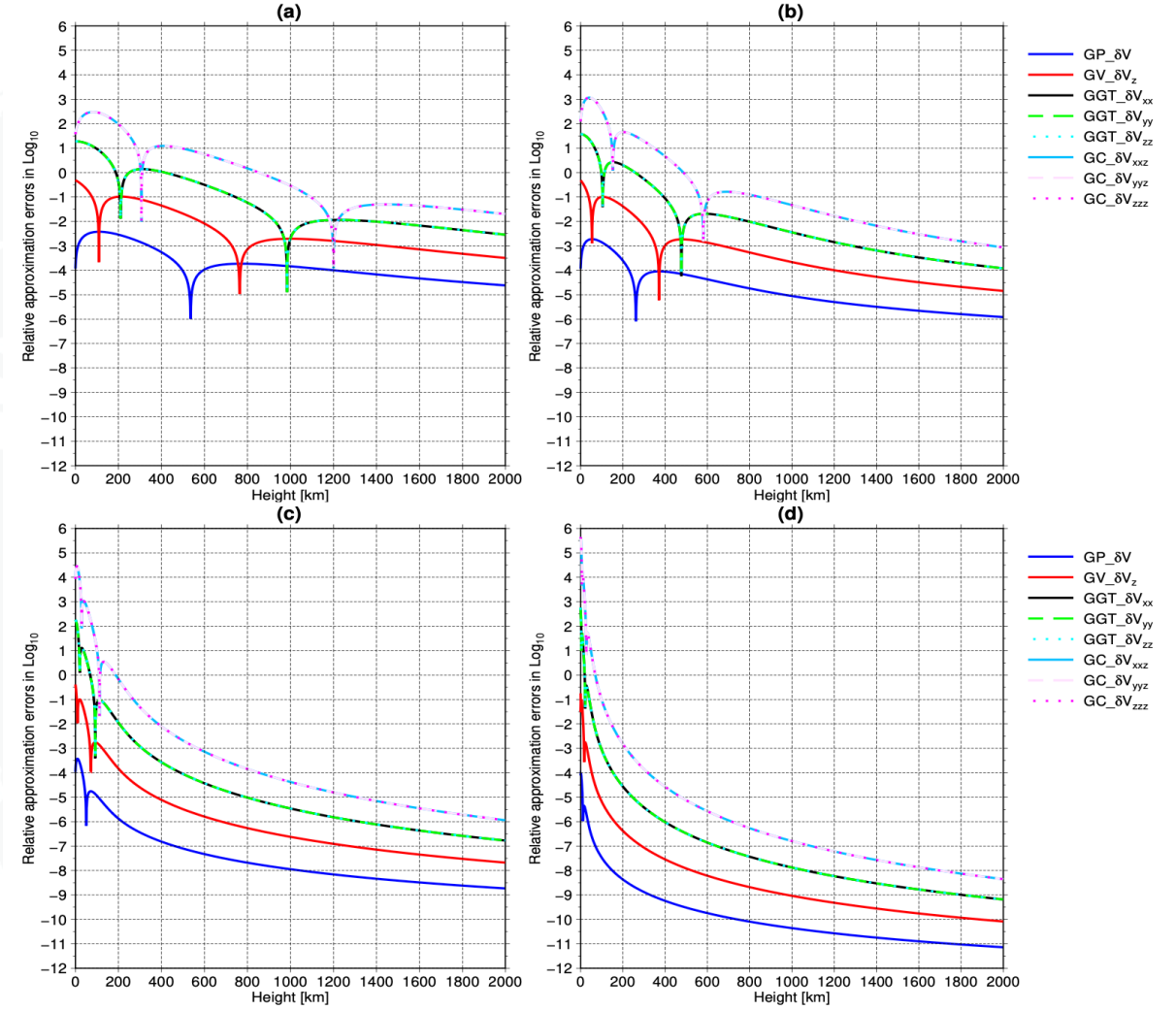


Fig. 5 Relative approximation errors in Log10 scale of nonzero gravitational effects of a **spherical shell** discretized using tessieroids with the influence of the computation point's height by a grid size of (a) 10d x 10d, (b) 5d x 5d, (c) 1d x 1d, and (d) 15'x15' in quadruple precision.

3. Numerical experiments

Table 3 Statistical information of the values in Fig. 4 for a **spherical zonal band**

Quantity	Grid size	Min	Max	Mean	STD
GP (δV)	$10^\circ \times 10^\circ$	-8.8	-3.6	-4.0	0.5
GP (δV)	$5^\circ \times 5^\circ$	-9.4	-4.5	-5.1	0.7
GP (δV)	$1^\circ \times 1^\circ$	-12.2	-7.0	-7.7	0.6
GP (δV)	$15' \times 15'$	-14.5	-9.4	-10.0	0.6
GV (δV_z)	$10^\circ \times 10^\circ$	-5.7	-2.6	-3.1	0.3
GV (δV_z)	$5^\circ \times 5^\circ$	-7.8	-3.5	-4.0	0.4
GV (δV_z)	$1^\circ \times 1^\circ$	-9.0	-5.9	-6.7	0.5
GV (δV_z)	$15' \times 15'$	-11.5	-8.3	-9.1	0.6
GGT ($\delta V_{xx}, \delta V_{yy}, \delta V_{zz}$)	$10^\circ \times 10^\circ$	-5.3	1.1	-2.3	0.6
GGT ($\delta V_{xx}, \delta V_{yy}, \delta V_{zz}$)	$5^\circ \times 5^\circ$	-6.5	0.6	-3.3	0.6
GGT ($\delta V_{xx}, \delta V_{yy}, \delta V_{zz}$)	$1^\circ \times 1^\circ$	-8.5	-2.9	-5.9	0.5
GGT ($\delta V_{xx}, \delta V_{yy}, \delta V_{zz}$)	$15' \times 15'$	-11.0	-4.6	-8.2	0.6
GC ($\delta V_{xxz}, \delta V_{yyz}, \delta V_{zzz}$)	$10^\circ \times 10^\circ$	-4.6	0.1	-2.0	0.3
GC ($\delta V_{xxz}, \delta V_{yyz}, \delta V_{zzz}$)	$5^\circ \times 5^\circ$	-6.8	-0.0	-2.9	0.4
GC ($\delta V_{xxz}, \delta V_{yyz}, \delta V_{zzz}$)	$1^\circ \times 1^\circ$	-8.0	-2.9	-5.4	0.4
GC ($\delta V_{xxz}, \delta V_{yyz}, \delta V_{zzz}$)	$15' \times 15'$	-10.3	-4.9	-7.8	0.4

Table 4 Statistical information of the values in Fig. 5 for a **spherical shell**

Quantity	Grid size	Min	Max	Mean	STD
GP (δV)	$10^\circ \times 10^\circ$	-6.0	-2.4	-3.8	0.6
GP (δV)	$5^\circ \times 5^\circ$	-6.1	-2.7	-4.9	0.9
GP (δV)	$1^\circ \times 1^\circ$	-8.7	-3.4	-7.6	1.1
GP (δV)	$15' \times 15'$	-11.1	-4.0	-10.0	1.2
GV (δV_z)	$10^\circ \times 10^\circ$	-5.0	-0.3	-2.5	0.9
GV (δV_z)	$5^\circ \times 5^\circ$	-5.2	-0.3	-3.4	1.1
GV (δV_z)	$1^\circ \times 1^\circ$	-7.7	-0.4	-6.1	1.5
GV (δV_z)	$15' \times 15'$	-10.1	-0.7	-8.5	1.6
GGT ($\delta V_{xx}, \delta V_{yy}, \delta V_{zz}$)	$10^\circ \times 10^\circ$	-4.9	1.3	-1.3	1.1
GGT ($\delta V_{xx}, \delta V_{yy}, \delta V_{zz}$)	$5^\circ \times 5^\circ$	-4.2	1.6	-2.2	1.4
GGT ($\delta V_{xx}, \delta V_{yy}, \delta V_{zz}$)	$1^\circ \times 1^\circ$	-6.8	2.3	-4.8	1.9
GGT ($\delta V_{xx}, \delta V_{yy}, \delta V_{zz}$)	$15' \times 15'$	-9.2	2.8	-7.2	2.0
GC ($\delta V_{xxz}, \delta V_{yyz}, \delta V_{zzz}$)	$10^\circ \times 10^\circ$	-3.9	2.5	-0.2	1.3
GC ($\delta V_{xxz}, \delta V_{yyz}, \delta V_{zzz}$)	$5^\circ \times 5^\circ$	-3.1	3.1	-1.0	1.7
GC ($\delta V_{xxz}, \delta V_{yyz}, \delta V_{zzz}$)	$1^\circ \times 1^\circ$	-5.9	4.5	-3.6	2.2
GC ($\delta V_{xxz}, \delta V_{yyz}, \delta V_{zzz}$)	$15' \times 15'$	-8.4	5.6	-6.0	2.4

- Mean values of the relative approximation errors in Log10 scale of the GP, GV, GGT, and GC for a **spherical zonal band** discretized using tesserooids with different grid sizes are **smaller** than those for a **spherical shell** discretized using tesserooids.

4. Conclusion

- The **simpler analytical expressions** for the radial GV and radial-radial GGT of a homogeneous spherical cap and spherical zonal band are derived. Moreover, we derive the **new analytical formulae of the GC** of a homogeneous spherical cap and spherical zonal band.
- Regarding the computation time and errors, **the benefit** of a spherical zonal band discretized using tesseroids is numerically confirmed in comparison with a spherical shell discretized using tesseroids.
- **A spherical zonal band discretized using tesseroids** can replace a spherical shell discretized using tesseroids in gravity field modelling in the future study.

5. Outlook

- The analytical solutions of gravitational effects of the spherical cap and spherical zonal band can be served as the reference values not only for tesseroids but also for **other spherical mass elements**.
- Research on the **higher-order gravitational potential gradients** of a spherical cap and spherical zonal band will be investigated based on the general formulae of Laplace's equation for higher-order gravitational potential gradient.
- The homogeneous density for the gravitational effects of a spherical cap and spherical zonal band will be extended to the **variable density**.
- Future research on the **direct comparison** between the spherical zonal band and spherical shell in the context of a practical application like residual terrain correction will be performed.
- Moreover, the theoretical expressions of **magnetic curvatures** and **higher-order magnetic potential gradients** of a spherical cap and spherical zonal band will be investigated in the near future.



Reference

- Deng XL, Shen WB (2018) Evaluation of gravitational curvatures of a tesseroid in spherical integral kernels. *Journal of Geodesy* 92(4):415–429
- Deng XL, Shen WB (2019) Topographic effects up to gravitational curvatures of tesseroids: A case study in China. *Studia Geophysica et Geodaetica* 63(3):345–366
- Heck B, Seitz K (2007) A comparison of the tesseroid, prism and point-mass approaches for mass reductions in gravity field modelling. *Journal of Geodesy* 81(2):121–136
- Lin M, Denker H, Muller J (2020) Gravity Field Modeling Using Tesseroids with Variable Density in the Vertical Direction. *Surveys in Geophysics* 41(4):723–765
- Papp G, Wang ZT (1996) Truncation effects in using spherical harmonic expansions for forward local gravity field modelling. *Acta Geod Geoph Hung* 31(1–2):47–66
- Wild-Pfeiffer F (2008) A comparison of different mass elements for use in gravity gradiometry. *Journal of Geodesy* 82(10):637–653



**Thank you
for
your attention!**